EL SEVIER

Contents lists available at ScienceDirect

Science of the Total Environment

journal homepage: www.elsevier.com/locate/scitotenv



Characterizing the diverse hydrogeology underlying rivers and estuaries using new floating transient electromagnetic methodology



John W. Lane Jr. ^a, Martin A. Briggs ^{a,*}, Pradip K. Maurya ^b, Eric A. White ^a, Jesper B. Pedersen ^b, Esben Auken ^b, Neil Terry ^a, Burke Minsley ^c, Wade Kress ^d, Denis R. LeBlanc ^e, Ryan Adams ^d, Carole D. Johnson ^a

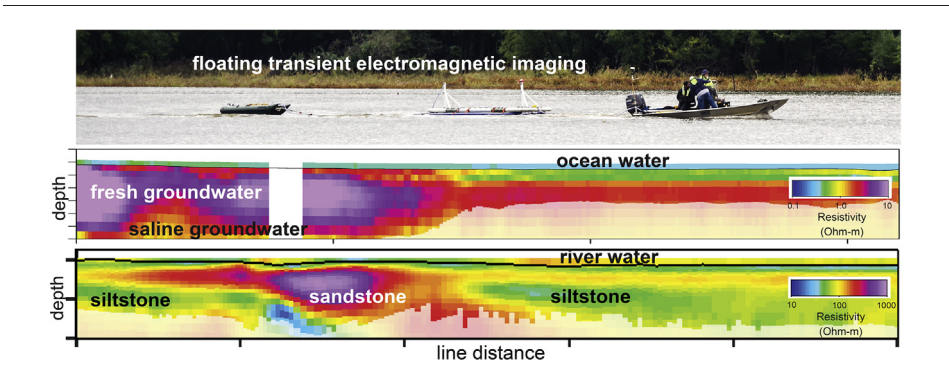
- ^a U.S. Geological Survey, Hydrogeophysics Branch, 11 Sherman Place, Storrs, CT 06238, USA
- ^b Institute of Geoscience, HydroGeophysics group, Aarhus University, Denmark
- ^c U.S. Geological Survey, Geology, Geophysics, and Geochemistry Science Center, USA
- ^d U.S. Geological Survey, Lower Mississippi Gulf Water Science Center, USA
- ^e U.S. Geological Survey, New England Water Science Center, Northborough, MA, USA

HIGHLIGHTS

The hydrogeology beneath large surface water features is often highly uniformed.

- Waterborne transient electromagnetic methods vastly improve existing capabilities
- Multi-scale geologic controls on groundwater/surface water exchange are characterized.
- Fresh/saline coastal groundwater interfaces are mapped in unprecedented detail
- Predictive models of water quality and supply will be improved by this new data type.

GRAPHICAL ABSTRACT



ARTICLE INFO

Article history: Received 17 April 2020 Received in revised form 4 June 2020 Accepted 6 June 2020 Available online 9 June 2020

Editor: Damia Barcelo

Keywords:
Hydrogeophysics
River
Groundwater
Saltwater intrusion
Groundwater/surface water interactions

ABSTRACT

The hydrogeology below large surface water features such as rivers and estuaries is universally under-informed at the long reach to basin scales (tens of km+). This challenge inhibits the accurate modeling of fresh/saline groundwater interfaces and groundwater/surface water exchange patterns at management-relevant spatial extents. Here we introduce a towed, floating transient electromagnetic (TEM) system (i.e. FloaTEM) for rapid (up to 15 km/h) high resolution electrical mapping of the subsurface below large water bodies to depths often a factor of 10 greater than other towed instruments. The novel FloaTEM system is demonstrated at a range of diverse 4th through 6th-order riverine settings across the United States including 1) the Farmington River, near Hartford, Connecticut; 2) the Upper Delaware River near Barryville, New York; 3) the Tallahatchie River near Shellmound, Mississippi; and, 4) the Eel River estuary, on Cape Cod, near Falmouth, Massachusetts. Airborne frequencydomain electromagnetic and land-based towed TEM data are also compared at the Tallahatchie River site, and streambed geologic scenarios are explored with forward modeling. A range of geologic structures and pore water salinity interfaces were identified. Process-based interpretation of the case study data indicated FloaTEM can resolve varied sediment-water interface materials, such as the accumulation of fines at the bottom of a reservoir and permeable sand/gravel riverbed sediments that focus groundwater discharge. Bedrock layers were mapped at several sites, and aquifer confining units were defined at comparable resolution to airborne methods. Terrestrial fresh groundwater discharge with flowpaths extending hundreds of meters from shore was also

^{*} Corresponding author. *E-mail address*: mbriggs@usgs.gov (M.A. Briggs).

imaged below the Eel River estuary, improving on previous hydrogeological characterizations of that nutrientrich coastal exchange zone. In summary, the novel FloaTEM system fills a critical gap in our ability to characterize the hydrogeology below surface water features and will support more accurate prediction of groundwater/surface water exchange dynamics and fresh-saline groundwater interfaces.

Published by Elsevier B.V.

1. Introduction

River corridors drain the landscape through a spectrum of hydrologic exchange processes and flowpaths that physically connect groundwater (GW) and surface water (SW) (Harvey and Gooseff, 2015). The spatial distribution of recharge and discharge within the riverine corridor is controlled in part by riverbed and bank geology (Winter et al., 1998); thus the physical structure and permeability of the riverbed is a critical component of GW/SW exchange processes (Bianchin et al., 2011). Because exchange processes are often critical to water quality (Boano et al., 2014), water supply (Wolock, 2003), and aquatic ecology (Poole, 2010), they are increasingly invoked in discussions of watershed management and restoration (e.g. Harvey et al., 2019; Hester and Gooseff, 2010). Although basin-scale numerical modeling capabilities for river-aquifer exchange have expanded (e.g. Bao et al., 2018; Dai et al., 2019), our ability to physically characterize the hydrogeology of river corridors at representative scales while maintaining spatial resolution has not kept pace. Therefore, most watershedto large basin-scale models of GW/SW connectivity are uninformed in the context of subsurface structure, particularly under larger rivers and estuaries.

Most existing methodologies to characterize the spatial and temporal hydrodynamics of GW/SW exchange were developed in headwater systems and intended for application at a series of "points" in space (Kalbus et al., 2006). In larger rivers, physical streambed point measurements are difficult to collect and may be impossible to scale up to system-representative information (Briggs et al., 2019). Difficulties in applying physical GW/SW methodology in large river systems forces a general reliance on net downstream change-based methodologies, for which, differences in river discharge and/or mixed water-column chemistry are evaluated along the river corridor and attributed to exchange processes. However, when using these methods, the underlying gross exchange processes remain ambiguous and impair prediction. Research has shown that gaining river corridors are likely to be influenced by 'legacy' groundwater contamination reflecting past land-use practices (Briggs et al., 2020; Sanford and Pope, 2013; Tesoriero et al., 2007), so the ability to identify and model specific GW/SW exchange dynamics is fundamental to improving contemporary water-quality management strategies. Additionally, in a time of baseline change, viable future predictions of river corridor dynamics are only possible if the fundamental dominant physical controls are well-characterized.

For these reasons, improved characterization methods are needed in order to design, calibrate, and test basin- to regional-scale predictive models. Of interest in larger order river systems are field methods able to inform groundwater-flow model structure (Dai et al., 2019), such as MODFLOW model (Harbaugh et al., 2000) estimates of the riverbed conductance parameter, a lumped term that includes streambed thickness and permeability, to which simulated dynamics of GW/SW exchange are highly sensitive. Airborne and near-surface hydrogeophysical methods complement more conventional river corridor field methodologies in evaluating the physical properties of the river corridor (Briggs et al., 2019; McLachlan et al., 2017; Minsley et al., 2012). For example, thermal infrared imaging can efficiently indicate zones of spatially preferential GW discharge across relatively large-scales based on watersurface temperature anomalies in summer and winter (Hare et al., 2015). Numerous studies have shown that electrical and electromagnetic methods are particularly useful to characterize geologic heterogeneity that controls GW/SW exchange zonation under lakes, streams, and rivers (Briggs et al., 2019; Day-Lewis et al., 2006; Parsekian et al., 2014; Toran et al., 2010) though surveys are often limited practically in spatial coverage and/or depth of bed penetration.

Electrical resistivity tomography is a common and robust geophysical approach used extensively for decades for mapping geologic structure, relative permeability and zonation in porewater electrical conductivity. The resistivity tomography method is most often used for land-based surveys but is also used in aquatic environments in a towed, continuous resistivity profiling (CRP) mode (e.g. Mast and Terry, 2019). For example, CRP has been used to map freshwater saturation in saltwater bay sediments (Manheim et al., 2004), and for estimating sediment thickness and locating faults (Kwon et al., 2005). CRP methods utilize a long floating electrode array (typically 30 to 100-m line) towed by a boat. Although the CRP method can provide highresolution resistivity models useful for delineating the hydrogeology under rivers and streams over substantial distances, practical limitations related to the length of the electrode array and a modest depth of investigation (DOI) limit application to large rivers and coastal settings. For example, Sheets and Dumouchelle (2009) were able to efficiently infer the spatial structure of permeable bed sediments along 20 km of a large river using continuous seismic, CRP and electromagnetic methods (EM), but the sub-bottom riverbed DOI was limited to approximately 5 m.

In general, EM techniques have been highly successful in mapping GW/SW interfaces when there are strong variations in either SW or GW electrical conductivity, providing natural tracers of subsurface flow. Although several instruments are limited to the close nearsurface (e.g. <10 m DOI), recharge of shallow groundwater from shallow lakes (e.g. Ong et al., 2010) and fresh GW discharge to rivers embedded in natural brines (e.g. Briggs et al., 2019) have been mapped over multiple-km scales with handheld frequency domain EM tools. Extraction of resources such as lithium from large scale natural brine systems is economically important (Munk et al., 2016), but pumping activities are likely to impact sensitive surface aquatic ecosystems (Marazuela et al., 2019). However, the complex hydrogeology and variable density flow of such systems requires next generation geophysical imaging techniques to validate predictive models (e.g. Marazuela et al., 2018) to better assess the impacts or resource extraction. Transient EM (TEM) system soundings have been used to map coastal saltwater intrusion over large areas to depths >100 m (Kalisperi et al., 2018), but data coverage is limited by the non-mobile data collection techniques.

To more effectively characterize larger order rivers and to work in more complex environments, there is a need for new geophysical methods with a significantly improved DOI and a substantially smaller towed instrument array length that also maintain high spatial resolution (e.g. meter's scale in the vertical). There is growing interest in the development and application of towed EM geophysical instruments, because towed methods can provide continuous subsurface information with high lateral resolution and a relatively large DOI. Mollidor et al. (2013) developed an in-loop transient EM TEM system and used it over a volcanic lake in Germany, in order to map underlying sediment thickness. Because the system used a large transmitter loop (18 $\,\mathrm{m}$ x18m), the authors encountered non-1D effects on the TEM data that could only be interpreted using a 3D EM modeling approach. Hatch et al. (2010) conducted a study comparing an airborne EM (AEM) survey to data collected with the towed in-loop TEM and direct current resistivity systems in the context of mapping spatially heterogeneous GW/SW connectivity in a saline aquifer system. They concluded that water-borne surveys have better lateral and vertical resolution compared to AEM but with limited DOI (~20 m). Recently, Auken et al.

(2019) presented a new ground-based towed transient electromagnetic system (tTEM) for rapid, efficient mapping of the subsurface, with high lateral and vertical resolution and DOI to 70 m. In this paper, we present a novel adaptation of the new tTEM system to open water to strengthen uninformed river corridor studies of GW/SW exchange dynamics. The boat-towed application of the tTEM system (called FloaTEM, i.e., floating tTEM) was applied in diverse hydrogeological settings of the United States including the Farmington River in Connecticut (4thorder stream), the Upper Delaware River in New York (5th-order stream), the Tallahatchie River in Mississippi (6th-order stream), and the Eel River estuary on Cape Cod, Massachusetts. For the Tallahatchie River case study, we include comparison to a land-based tTEM survey to demonstrate how riverbed geology is tied to the adjacent floodplain landscape. Data are compared to existing geological logs where available to aid in the hydrogeological interpretations. As mentioned above, geologic data are rarely available directly below larger surface water bodies, so we use forward modeling techniques to predict FloaTEM system responses to complicated riverbed electrical conductivity structures. Waterborne geophysical imaging of streambed sediments is always impacted by the surface water layer, so forward modeling was also used to test the system under varied water column thickness to assess how deployment over deeper water might influence the ability to resolve discrete streambed features. For the Tallahatchie River case study we compare our FloaTEM results directly to existing AEM data, and for the Eel River case study we compare to existing CRP data, to investigate the relative strengths of FloaTEM compared to existing geophysical methodology. Our combined synthetic and field datasets demonstrate how the FloaTEM method fills a critical gap in our ability to resolve the physical structure of large riverbeds and map saline groundwater interfaces, likely facilitating improved estuary- and basin-scale predictive model development and calibration. Although the FloaTEM concept is demonstrated here with Aarhus technology, the concept is transferable to other transient electromagnetic systems with similar specifications.

2. Methodology

Here we describe the towed FloaTEM system, field data analysis and inversion, and forward modeling of expected sensitivity in resolving varied large river hydrogeologic scenarios.

2.1. FloaTEM system

The FloaTEM system uses an offset-configuration loop consisting of a single-turn, 4 m \times 2 m transmitter (Tx) loop and a 0.56 m by 0.56 m multi-turn receiver (Rx) coil with an effective area of 5 m². The offset distance between the center points of the Tx and Rx loops is 9 m, with the Tx and Rx coils affixed to pontoons and a small rubber raft, respectively. Fig. 1 shows side and plan views of the system configuration. The system is towed by a boat containing the TEM transmitter, control unit, and receiver electronics at a speed of approximately 10–15 km/h. A water depth sensor is included in the instrument data acquisition system and those data are used to constrain the thickness of the water column during inversion, enhancing the resolution of shallow bed sediments that often impart strong control on GW/SW exchange patterns. For the case studies presented here a depth transducer transmitting at 200-kHz and sampling at 5 Hz (CEE Echo, CEE HydroSystems) was placed at the boat stern and used to track water depth (bathymetry). Additionally, a water-quality probe (YSI ProDSS Multiparameter Water Quality Meter) is used to acquire georeferenced surface water electrical conductivity (EC) values every 30 s along the profile. The EC data are used for general survey reference, but not explicitly included in the data inversion process. For data positioning, two GPS receivers are mounted on the system, one at the TX-coil and another directly above the echo sounder. All data are collected and timestamped by the FloaTEM computer that also collects the TEM data and runs the navigation system.

2.2. Data acquisition

The data acquisition system uses dual-moment measurements, transmitting a low-moment and a high-moment current pulse to obtain both shallow and deep subsurface information. For FloaTEM, the low-moment pulse transmits 2.8 amperes (A) into the Tx coil with a turn-off time of 2.6 (microsecond) μ s, with the first usable time-gate centered around 4 μ s (time from the beginning of the turn off ramp); whereas the high moment pulse transmits 30 A into the Tx coil. The repetition frequencies for the low-and high-moment pulses are 2160 and 660 Hz, respectively.

The land-based tTEM unit uses the same transmitter and receiver as the FloaTEM, however the transmitter and receiver are mounted on sleds at a height of about 0.5 m above the land surface and towed by an all-terrain vehicle at speeds of 10–15 km/h. Airborne EM data were acquired with the Resolve (CGG Airborne) frequency-domain instrument over the same reach of the Tallahatchie River as the FloaTEM as part of a larger mapping campaign in the region. The AEM data comprise five horizontal coplanar Tx-Rx coil pairs separated by about 7.9 m at frequencies between 383 and 133,528 Hz, and one vertical coaxial coil pair separated by about 9 m that operates at 3315 Hz. Nominal system height above ground, or river, surface is 30 m and is recorded along flight paths. System parameters for this survey are the same as reported by Thompson Jobe et al. (2020).

2.3. Processing and inversion

Processing of FloaTEM data follows the approach presented by Auken et al. (2009) for airborne transient EM data, performed here using Aarhus Workbench software (www.aarhusgeosoftware.dk). The processing steps of FloaTEM data consist of 1) pre-processing to identify and remove data clearly impacted by capacitive coupling to civil infrastructure (e.g. power lines, fences, buried pipes, etc.), 2) averaging raw TEM sounding data over approximately 3 second time windows to suppress random noise, resulting in a depth-dependent running mean used to populate each TEM sounding spaced approximately 10 m apart along data-collection track lines (assuming an average boat speed of 10 km/h), 3) preliminary inversion using a 1D laterallyconstrained inversion (LCI) scheme to assess the quality of preprocessing, and examine areas along the profile with high data misfit to determine if additional data are impacted by coupling and, if necessary, removed, and 4) final LCI inversion. Although the LCI inversion approach breaks the data collection longitudinal profiles into a series of 1D models for efficiency, lateral information from adjacent data are used to constrain each 1D inversion (Auken et al., 2015), which improves the stability of the inversion. A 1D modeling assumption may not be appropriate in cases where there is significant lateral variation in EM properties, given that the true sensitivity pattern of TEM instrumentation is a 3D volume. However, we note that the FloaTEM system has a relatively small sensitivity footprint in shallow sub-surface compared to airborne and other ground-based system (Madsen et al., 2017). In addition, we note that truly 2D or 3D inversion problems at the scale of interest here (e.g., ~meter resolution over tens of km distances) would likely be computationally impractical with modern consumer-level computer resources.

The forward response of the TEM data incorporates the modeling of the key parameters of the tTEM system such as transmitter waveform, transmitter/receiver timing, receiver-coil's finite bandwidth, receiver low-pass filter, receiver front-gate, gate widths, and system configuration. All FloaTEM data were inverted using a smooth layer model consisting of 25 layers with depth to layer boundaries ranging from 0.5 m to 120 m. Logarithmic incremental layer thicknesses are set in defining the 1D model discretization. Inversions discussed here were

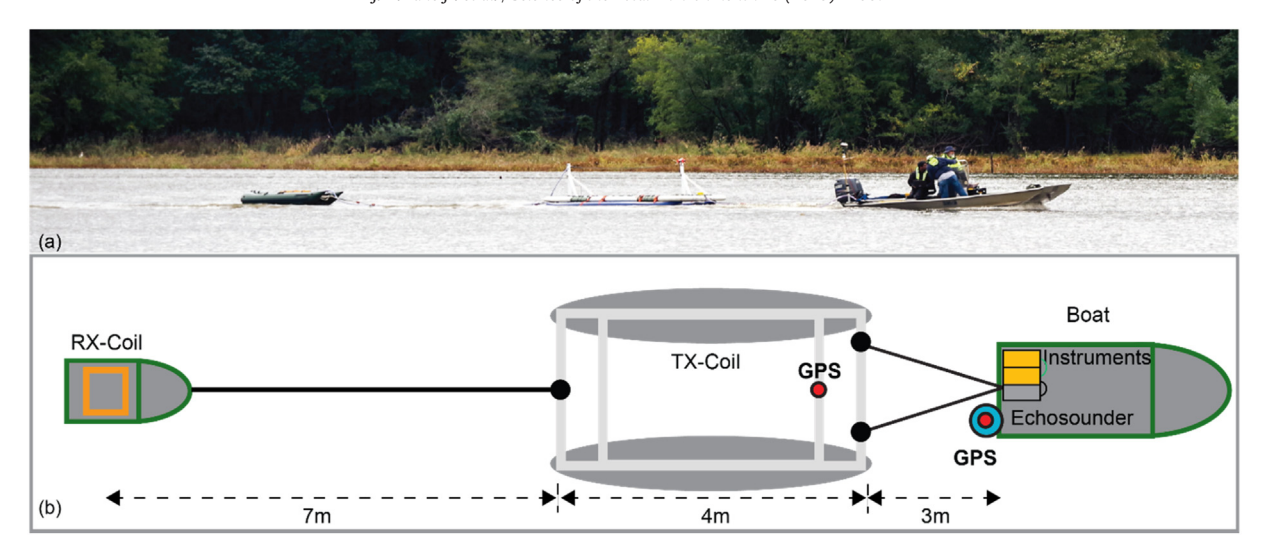


Fig. 1. The FloaTEM system in side (a) (photo credit to Shane Stocks, USGS) and (b) plan views. Rx-Coil indicates the receiver coil and Tx-coil indicates the transmitter coil fixed to a rubber boat and pontoons, respectively. The approximate towed footprint behind a motorized watercraft is shown in the bottom schematic.

carried out using the water-depth data as a constraint on the top layer (surface water) thickness using the Workbench software when those data were available from the onboard echo sounder. This measured surface water depth constraint serves to enhance the resolution of the top 5 m of streambed resistivity, which a critical physical control on GW/SW exchange. The expected DOI for the inverted profiles was calculated in Workbench for each model, following methods described by Christiansen and Auken (2012).

2.4. Forward modeling

Discrete zones or layers of relatively high-permeability riverbed sediments have been shown to control large-scale GW/SW exchange (Slater et al., 2010), assuming the permeable zones are not 'capped' by lower permeability fines that tend to accumulate in larger rivers and estuaries (Bianchin et al., 2011). The ability of the FloaTEM system to detect hydrogeological variations below a large river was evaluated through forward modeling exercises carried out with the AarhusInv forward/inverse modeling software (Auken et al., 2015). We first evaluated the ability of the FloaTEM system to detect semi-confining less permeable deposits in the riverbed, which may play an important role in regulating GW/SW exchange. In this exercise, we defined electrical resistivity for the water column (50 Ω -m), permeable sand and gravel deposits (500 Ω -m), and less permeable clay (20 Ω -m) based on ranges reported in Palacky (1988). For the forward modeling scenarios, the water-column thickness was varied between 3 and 30 m, and the modeled thickness of the layer of clay at the riverbed interface was increased from 1 to 10 m to test a range of potential field conditions.

Time domain electromagnetic data (voltages from 35 high-moment time gates and 45 low-moment gates) were simulated in AarhusInv over a 1D layered model. Simulations were performed using the configuration settings of the FloaTEM system. A noise floor value of 10^{-9} V ampm $^{-2}$ plus random Gaussian noise of 5% was applied to the simulated data. LCI 25-layer inversions (the same as used for field data in this manuscript) were carried out on the noise-contaminated data in AarhusInv. Layers within the water column were fixed in the inversion, given our real expectation that water-column thickness and electrical conductivity will be reasonably well quantified during field data collection.

3. Results and discussion

FloaTEM electromagnetic imaging surveys were conducted between October and December 2018 in a range of riverine settings across the United States including 1) the Farmington River, near Hartford, Connecticut; 2) the Upper Delaware River near Barryville, New York; 3) the Tallahatchie River near Shellmound, Mississippi (includes land-based towed-TEM); and, 4) the Eel River estuary, on Cape Cod, near Falmouth, Massachusetts. A range of geologic structures and pore water salinity interfaces were identified yielding new insight into hydrogeologic processes that impact GW/SW exchange beneath large waterbodies. Additionally, precisely known large river hydrogeologic scenarios were explored using forward modeling.

3.1. Forward modeling results

Inverse results from the forward modeling are shown in Fig. 2. River depths of 3, 10, and 30 m were modeled with clay ranging from 1 to 10 m in thickness. For our hypothetical river system and modeled electrical resistivities, the AarhusInv results suggest clay thicknesses >2, 2, and 3 m for river depths of 3, 10, and 30 m, respectively, can be resolved by the FloaTEM system. Therefore, although the presence of any clay in these forward models impacts the resulting inversion images, there is likely little ability to confidently map a clay/fines streambed interface cap <2 m in thickness with the FloaTEM system. For deep water (up to 30 m) this minimal quantifiable thickness of clay increases >3 m under the conditions tested.

Additional modeling was conducted to assess the performance of the FloaTEM system in more complex hydrogeologic environments as shown in Fig. 3. For this exercise, we assume a 10-meter water column thickness and similar resistivity values for the hydrogeological units as we did for the clay-cap models, with the addition of an intermediate resistivity (200 Ω -m) glacial till deposit. Discrete, low resistivity lenses (resistivity = 20 Ω -m; simulating silt/clay) approximately 100-m long by 10-m thick were embedded in the domain. We utilized the same forward-inverse modeling procedure. The forward-modeling results show the structure associated with the major sands and gravels and glacial till units and delineate the six clay lenses (Fig. 3b); deeper low-resistivity clay lenses are less well-resolved compared to those at the riverbed interface. The deep clay lens embedded within the glacial till is the most poorly resolved owing to the reduced electrical contrast between the lenses and the matrix.

The results of the forward modeling exercises indicate great potential but also identify practical limitations of the FloaTEM method in resolving the complex hydrogeology beneath larger water bodies. The system should be able to delineate relatively high conductivity zones, representative of either fine-grained sediments or clays, provided

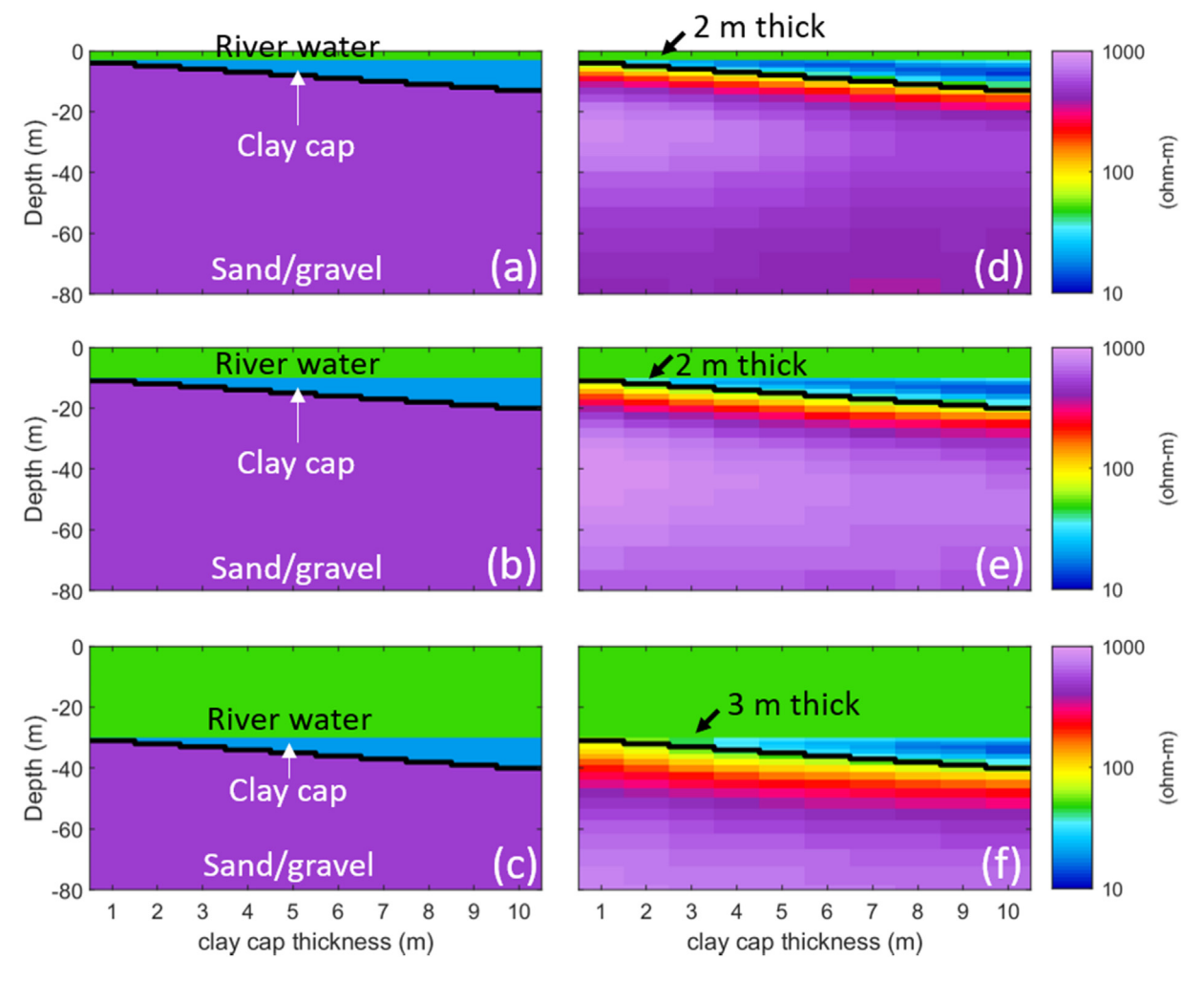


Fig. 2. Aarhuslnv modeling to assess the ability of the FloaTEM system to resolve layers of less permeable material (a-c) true models of electrical resistivity for a water column of 3, 10, and 30 m and a layer of clay ranging from 1 to 10 m in thickness; (d-f) corresponding inversion results indicating potential FloaTEM system response to less permeable clay. Thickness of minimum resolvable layer is indicated by black arrows.

these zones are of sufficient size, depth, and electrical contrast with respect to the surrounding material. Further, our modeling indicates that we will be able to identify features at the reach to groundwater model scale for a reasonable range of subsurface geoelectrical conditions and river depths. We note the high lateral resolution of the clay lenses is explained by the relatively small footprint of the towed system.

3.2. Farmington River (4th-order stream)

The Farmington River watershed (1571 km²) spans northwestern Connecticut and southwestern Massachusetts. The Farmington River discharges to the Connecticut River, which is a major source of nutrients and contaminants to Long Island Sound, contributing to summer coastal

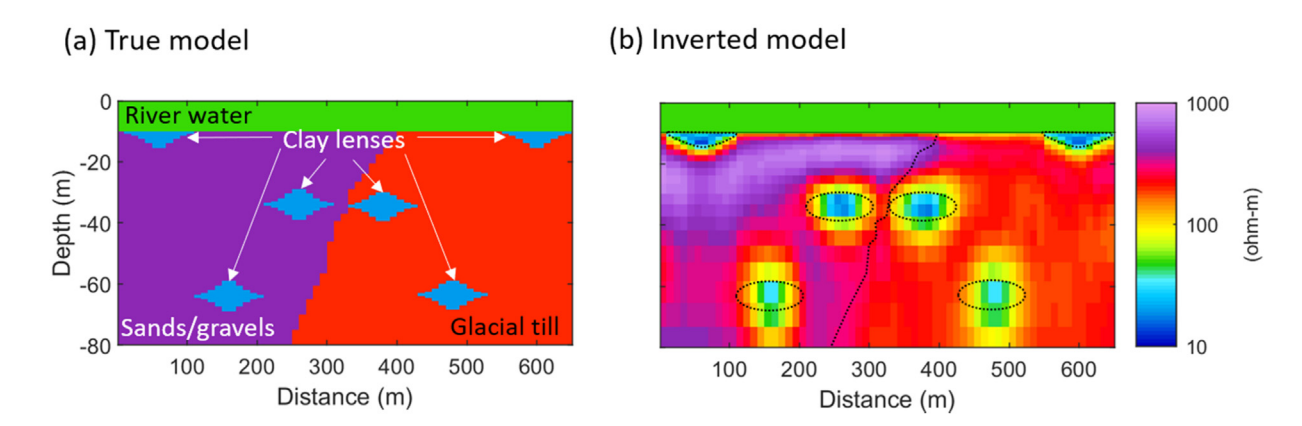


Fig. 3. Forward/inverse modeling to assess the performance of the FloaTEM system to resolve hydrogeological features that possess electrical contrasts; (a) true model for which FloaTEM data were simulated; (b) recovered model from inversion; feature boundaries are overlain as dotted black lines.

eutrophication. The Farmington River watershed has experienced substantial changes in land cover over the last several decades owing to the transition from agricultural to suburban development. It is thought this shifting legacy of land use may contribute to nutrient loading of the river via the GW flowpaths to numerous major GW discharge zones along the river corridor, and that these major discharge zones are controlled in part by river corridor geology (Barclay, 2019). Principal bedrock aquifers in the Farmington River watershed are the New England crystalline-rock aguifer and the Mesozoic sandstone and basalt aguifer of the Newark Supergroup (Olcott, 1995). Bedrock is overlain by glacial till across most of the watershed, with areas of valley-fill stratified-drift aquifers (Soller et al., 2012), resulting in a wide range in surficial sediment hydraulic conductivity and related GW connectivity with the river. The river length mapped for this case study connects an arkose (lower Portland Formation) bedrock-lined river section with variable thin alluvial cover to the north with the 234-acre Rainbow Reservoir (built in 1925) section with thick fine sediment accumulation to the south. In the study area, the river runs slightly oblique to bedrock strike over dipping beds of sandstone interbedded with finer-grained siltstone.

On November 15, 2018 about 5.6 km of Farmington River length were mapped with FloaTEM (White et al., 2020) (Fig. 4a). Along this study reach, data were collected in subparallel lines along opposite banks of the Farmington River from an upstream river island down to the impounded Rainbow Reservoir. Water depth data were collected over most of the data track lines, though the echo sounder malfunctioned over some short sections (Fig. 4b,c). The data collection lines are plotted in map view by inversion model residuals (Fig. 4a), which were generally higher in zones of higher streambed resistivity and were not noticeably impacted by the direction of boat travel against the current (Fig. 4a). The residuals presented here are normalized chisquared errors from the inversion, with values of 1 or less indicating that the inversion was able to fit a model to data within the expected distribution of data errors. Toward the upstream (western) end of the study reach, FloaTEM Line 130 follows the main channel whereas Line 120 follows a large side channel to the south of a river island (Fig. 4b, c). The landward banks on both sides of the island are lined with clusters of preferential GW discharges as identified with thermal infrared observations by Barclay (2019). Bank sands and gravels in these seepage zones were observed to overly shallow bedrock, and the main river channel is scoured to bedrock for a few hundred meters downstream of the island. The FloaTEM inversion from Line 120 along the side channel section where GW discharges were most concentrated shows a strongly resistive zone just below a resistive riverbed, interpreted as gravels over sandstone bedrock, consistent with visual observations (Fig. 4c). This combination of high permeability glacial deposits over shallow bedrock is a known driver of GW discharge (Winter et al., 1998). The main channel upstream section shown in Line 130 also shows a near-surface resistive zone, though there is indication of greater accumulation of lower-resistivity alluvial sediment in that area

Other large-scale features visible along both data collection lines are apparently dipping resistive bedrock layers consistent with the geologic mapping described above. These resistive units occur in discrete sections along the profile with apparent dip angles to the east (apparent as the river does not flow normal to strike in this area) and may reflect layers of sandstone interbedded with less-resistive silt-rich bedrock. The apparent dip angle is more evident when the FloaTEM data inversion is viewed without vertical exaggeration, such as the subsection of Fig. 4d, corresponding to a zone where the river narrows as it crosses a sandstone bedrock layer. Farther downstream along the reservoir section surface water depth increases (Fig. 4b, c) and is underlain by several meters of the least-resistive streambed interface sediments observed along the study reach, indicating accumulation of alluvial fines in slower flowing water. This finding is consistent with visual observations made by boat when the reservoir was partially drained in 2017

when extensive deposits of fine-grained sediments and organic deposits were noted along the reservoir bed. These low-resistivity fines appear to overly resistive bedrock along the reservoir section of Line 130, though unlike the upstream island scenario of coarse material over shallow bedrock, the fine alluvial sediments likely act as a cap to inhibit GW/SW exchange in this deeper water. Based on the forward modeling scenarios using similar surface water depths (Fig. 3b) the thickness of this cap layer is likely >2 m to be captured by FloaTEM.

3.3. Upper Delaware River, New York and Pennsylvania (5th-order stream)

The Delaware River's upper basin lies within the Glaciated Low Plateau section of the Appalachian Plateaus province. In the study area, the Upper Delaware cuts a narrow valley through sandstone bedrock of Devonian age along the border between New York and Pennsylvania. Bedrock is exposed along the streambed in isolated areas though there are also thick glaciofluvial deposits consisting of outwash sand and gravel and ice-contact sand, gravel, and silt particularly on the inside of meander bends and where larger tributaries empty into the river. Evidence of such deposits is shown by USGS boring 12008-14 (https://txdata.usgs.gov/GeoLogArchiver/odata/Logs(31076)/LogFile?_=1590785864403) that penetrates approximately 20 m of glaciofluvial deposits above bedrock (Fig. 5).

On December 6, 2018 FloaTEM data were collected over approximately 64-km of river length over 2 days using a jetboat to tow the system, though only 10.4-km are shown here, starting just downstream of the Lackawaxen River confluence (White et al., 2020). The DOI calculated for this section was spatially variable, but typically extended to at least 21 m below the streambed interface. Several sections of data were removed before performing the inversion due to (coupled 'powerline' data) interference with human infrastructure along this populated section of river. The 25-layer laterally constrained inversion model residuals were typically <2 (unitless metric) but increase toward the downstream end of the line. Generally, this section of riverbed shows resistive sediments (approximately 600–900 Ω -m) interpreted as sand and gravel overlying a more resistive transition (>1000 Ω -m), which is interpreted as the sandstone bedrock contact. The inferred bedrock contact shallows in several places to within 6 m of the streambed interface, which is consistent with the known geology of the Upper Delaware River, though in other places the resistive transition occurs at >25 m depth. There are several obvious low-resistivity zones in the streambed that extend 100's of m in length and may reflect alluvial sediments with higher silt content that would inhibit GW/SW exchange. A comparison of the FloaTEM inversion to the adjacent USGS Boring 12008-14 supports the interpretation of a predominance of sand and gravel deposits with interbedded siltier zones overlying sandstone

Previous GW/SW exchange characterization related to endangered dwarf wedgemussel habitat along a similar upstream stretch of the Upper Delaware River indicated that focused zones of groundwater discharge create important aquatic habitat niches in this system (Briggs et al., 2013), though efforts to explain the occurrence of discharge zones based on near-surface geology were hampered by the limited depth of investigation (i.e. <5 m) of other towed EM tools (Rosenberry et al., 2016). The streambed resistivity structure mapped with FloaTEM over this 10.4-km track line indicates variable depth to bedrock and large-scale (100's of m in length) silt-rich zones. A shallowing of the bedrock contact is known to force lateral down-valley groundwater flowpaths toward the surface, causing GW/SW exchange (Winter et al., 1998), while inclusion of silt into sand and gravel pore spaces is likely to decrease hydraulic conductivity and also force spatial variability in groundwater discharge (Nyquist et al., 2008; Rosenberry et al., 2016). Therefore, this proof of concept study indicates FloaTEM data may be particularly useful for groundwater-dependent habitat assessments in the Upper Delaware River related to the dwarf wedgemussel and managed recreational cold-water fishes.

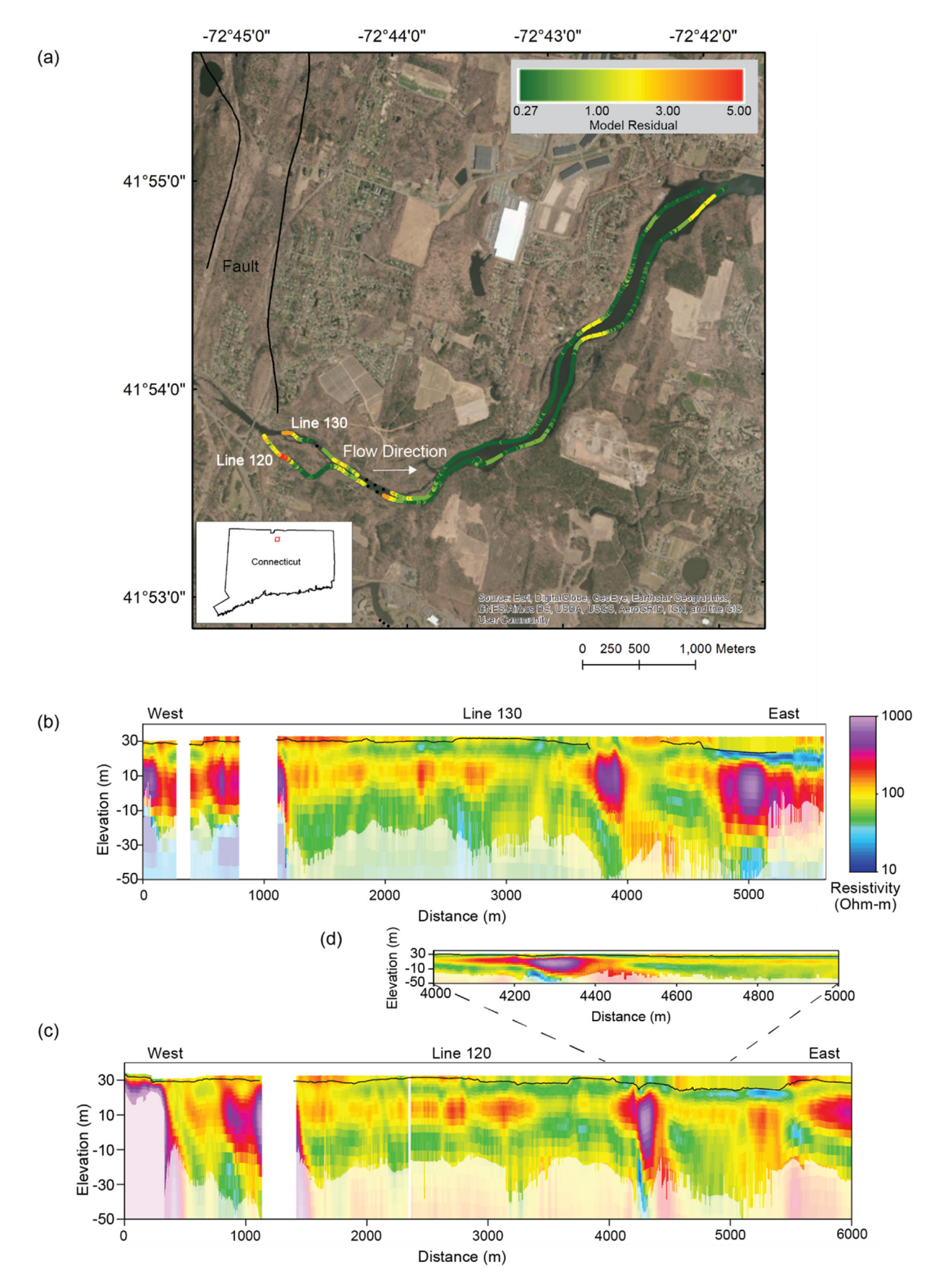


Fig. 4. The FloaTEM survey track line is plotted using inversion model data residuals in map view (a). Inverted resistivity sections from Line 130 (b), Line 120 (c) are shown and white space gaps in the profiles indicate areas where infrastructure-coupled data were removed from profiles. Panel (d) shows a subset of Line 120 without vertical exaggeration where the apparent dip of the sandstone bed is not distorted. The black line along the inversion sections indicates the streambed interface below the surface water column.

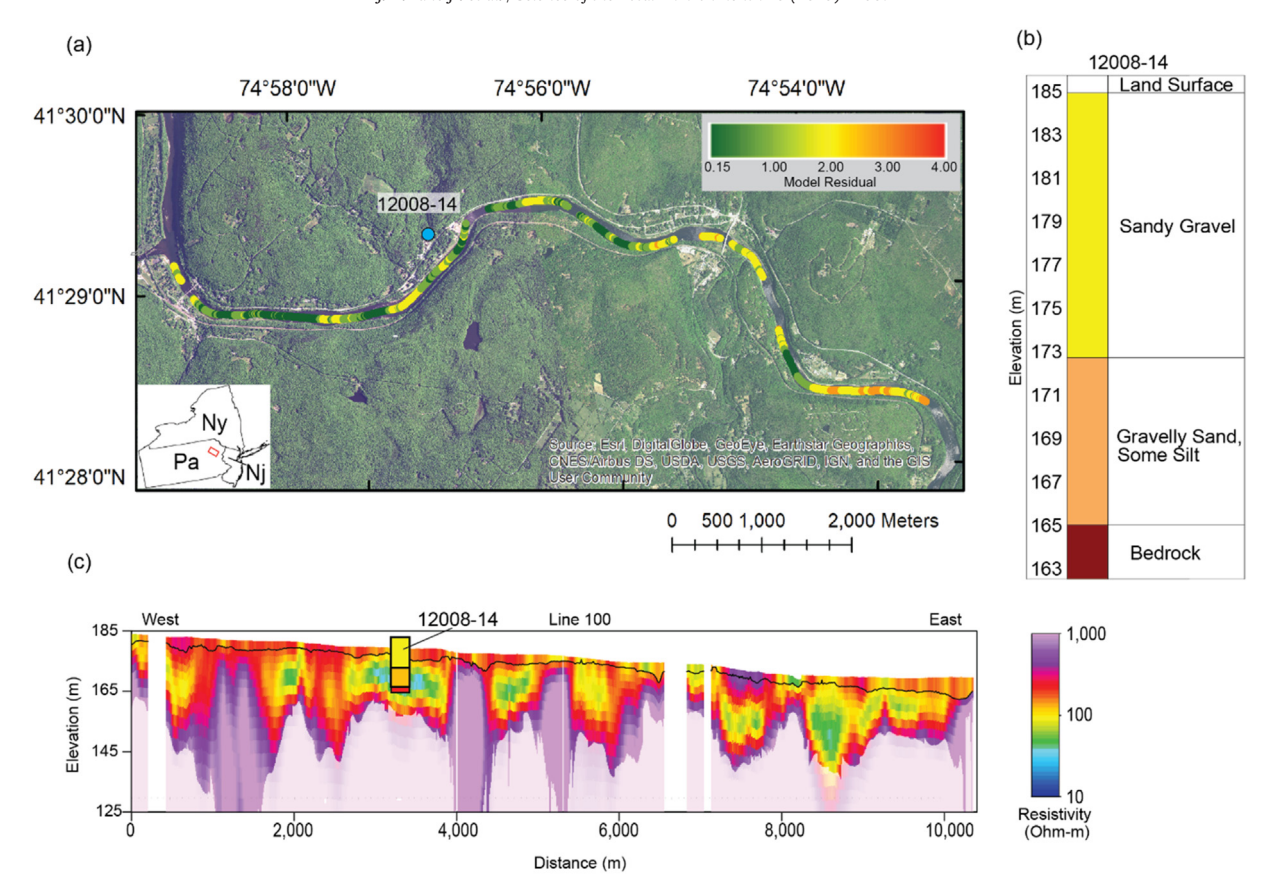


Fig. 5. The 10.4-km track of the FloaTEM instrument Upper Delaware River channel is shown using inversion model residuals plotted in map view (a), known adjacent borehole lithology (b), and inverted resistivity section from the Delaware River surveys near Barryville, NY (c).

3.4. Tallahatchie River (6th-order stream)

The Mississippi Alluvial Plain (MAP) is one of the most important agricultural regions in the United States, and crop productivity relies on groundwater irrigation from a hydrogeologic system that is poorly defined. Agricultural water use from in MAP has resulted in substantial groundwater-level declines and reductions in river baseflow. Current research to better constrain paired aquifer and river dynamics couples numerical groundwater modeling with uncertainty-targeted, geophysical surveys to improve the characterization of the alluvial aquifer system (Kress et al., 2018). The better-informed numerical groundwater model could then be used to predict potential future effects of wateruse changes, climate change, conservation practices or the construction of diversion-control structures to help manage the water resource. Understanding the areal and vertical distribution of coarse- and finegrained materials is important to improve regional and local groundwater models and inform estimates of recharge potential under natural and engineered conditions within the MAP aquifer system.

Air-, water-, and land-based geophysical methods were collected in support of the framework component of the MAP study. Extensive AEM surveys using the Resolve frequency-domain electromagnetic system were conducted in multiple phases, including a high-resolution grid of flights near the Tallahatchie River study area from late February to early March 2018 (Burton et al., 2020), and a large regional survey of the entire MAP region, including the river profile shown here (White et al., 2020), from November 2018 through February 2019. During October 2018, approximately 150 km of FloaTEM data were collected on Mississippi and Louisiana waterways, and approximately 36.5 km of tTEM data were collected on land at two locations in March 2018 (White et al., 2020), in west-east profiles separated approximately 20 m apart in association with an extraction and infiltration

investigation. In the focus area presented here, the uppermost 40 m comprises sands of the shallow Quaternary Mississippi River Valley alluvial aquifer system. Beneath the surficial aquifer, from depths of approximately 40–80 m, the Middle Claiborne aquifer consists of a mix of sand, silt, and clay. Below depths of about 80 m, there are clay and silt deposits of the Lower Claiborne confining unit (Fig. 6b) (Hoffmann, 2017).

In addition to plotting the course of an 18.3 km section of the FloaTEM survey (A–A′), Fig. 6a shows the model inversion residuals. The residuals are generally close to 1, indicating a good fit in inverted data with respect to the observed data. As with the other case studies zones that showed obvious interference with infrastructure were removed from the FloaTEM dataset before inversion. The tTEM data collected adjacent to the river also had low model residuals. An AEM profile (Fig. 6c) was acquired along the same reach of the Tallahatchie River, following a similar path as the FloaTEM survey (Fig. 6d). The inverted resistivity cross sections are similar in distribution of resistivity along the profiles, in magnitude, and location of discrete features though the data density of the FloaTEM system was higher resulting in sharper boundaries on discrete conductive features. The AEM had a DOI of about 80 to 90 m and the FloaTEM had a DOI of 80 to 100 m. The tTEM had a reduced DOI that varied from 10 to 50 m and overall the land-based profile was more electrically resistive than the adjacent river lines (Fig. 6e). The relatively shallow tTEM DOI at the southern end of the profile is caused by the removal of late-time gates coupling to nearby powerlines to the south.

The collective FloaTEM/AEM surveys (A–A′) at Shellmound indicate high resistivity zones correlate with coarse-grained materials (sand and gravels) consistent with the Mississippi River Valley alluvial aquifer, and low resistivity materials with finer-grained sediments (silts and clays), which are consistent with overbank materials and with the Lower Claiborne confining unit and portions of the Middle Claiborne aquifer.

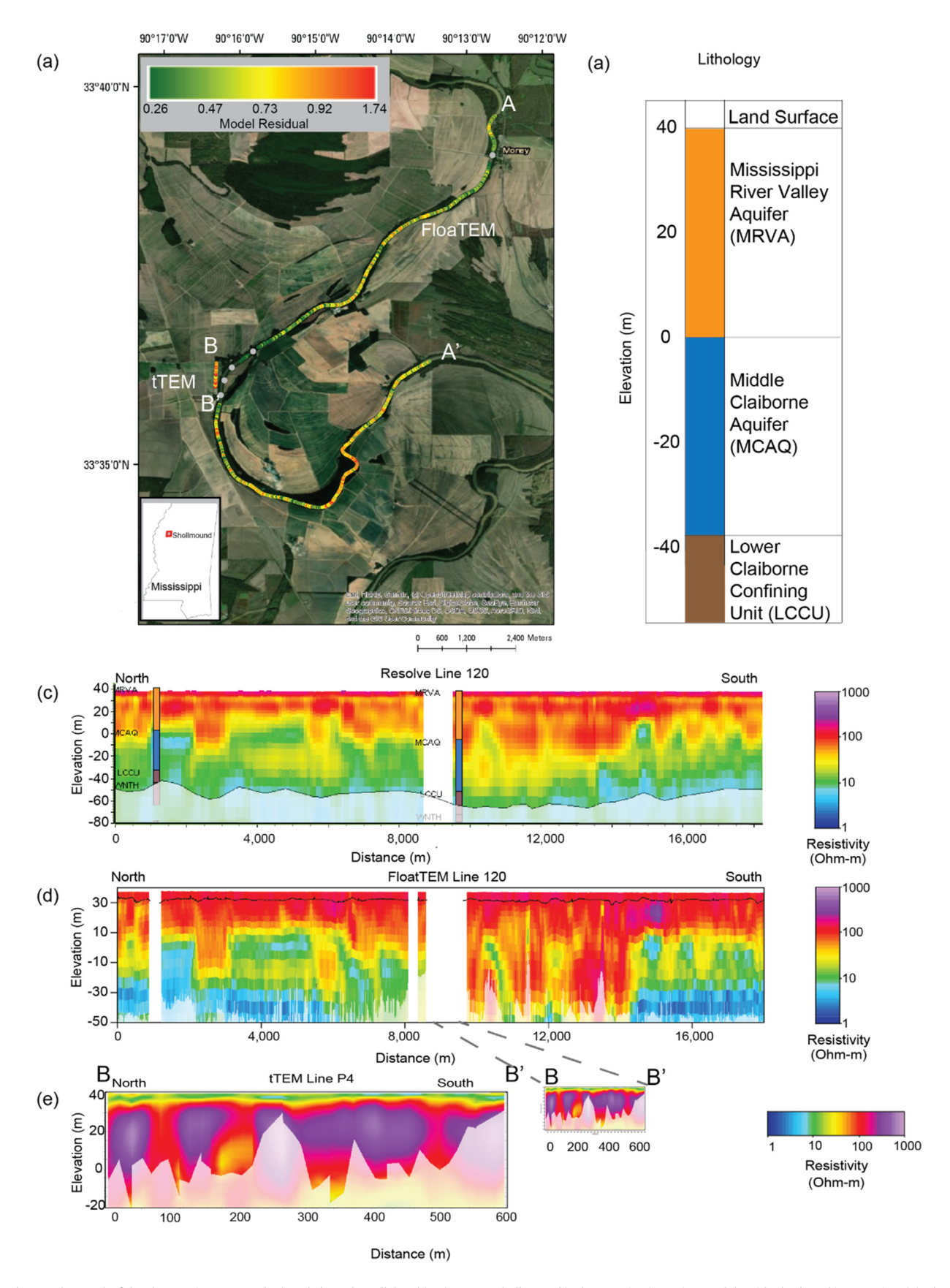


Fig. 6. The 18.3-km track of the FloaTEM instrument deployed along the Tallahatchie River near Shellmound is shown using inversion model residuals plotted in map view (a), along with known lithology (b), and inverted resistivity sections from paired AEM (c), and FloaTEM (d). Additional, land-towed tTEM data collected across a nearby field are shown (e).

The high resistivity zones lining and below the streambed indicate the potential for recharge to the aquifer from the river in those zones through coarser alluvial material. Identifying locations where there is potential for recharge to the aquifer through streambed infiltration and identifying locations where infiltration is blocked by impermeable or less permeable clay and silt layers is important for groundwater model input. A smaller 100-m scale resistive feature at approximately 15 km along the FloaTEM line just below the sediment-water interface may represent a paleochannel filled with particularly coarse bed material that would provide a conduit for subsurface flow and GW/SW exchange. In addition, the distribution of resistivity with depth can be helpful for framework characterization and groundwater model development.

3.5. Eel River estuary

The Eel River estuary is one of a series of narrow saltwater estuaries and intervening narrow peninsulas along the Nantucket Sound coast of southwestern Cape Cod, Massachusetts (Howes et al., 2013). The tidal river extends about 3 km inland from the barrier beach along the Sound and is about 30 to 200 m wide and 1 to 2 m deep. A densely populated peninsula with single-family homes on septic systems borders the embayment on the east (Fig. 7a), a more detailed description of the area can be found in Colman et al. (2018). Fine-grained organic sediments on the estuary bottom are expected to be underlain by about 100 m of glacial sand, gravel, silt, and clay that overlie granitic bedrock (Hull et al., 2019). The narrow bays occupy flooded erosional valleys cut into the Cape Cod glacial outwash plain at the end of the Pleistocene Epoch. Farther inland similar erosional valleys serve as groundwater drains for the regional aquifer (Uchupi and Oldale, 1994), with average yearly base-flow contributions exceeding 90% (Briggs et al., 2020). Fresh terrestrial groundwater from the unconfined Cape Cod aquifer discharges along the Eel River from inland areas and the adjacent peninsulas. However, the fine-grained, low permeability marine sediments in the estuary combined with the difficulty in making direct groundwater discharge measurements strongly complicates any interpretations and predictions of fresh groundwater discharge along the Eel River estuary. In contrast to the other three case studies, spatial variation in subsurface resistivity along the Eel River FloaTEM data collection line is expected to be most directly related to the variation in pore water resistivity at the terrestrial/marine GW interface.

On November 28, 2018, approximately 1.6 km of FloaTEM data were collected along a north-to-south track line from the narrow northwestern branch of the embayment to a point just inside the barrier beach at Nantucket Sound (White et al., 2020). Although infrastructure typical of residential suburban development is prevalent along the shoreline in this area, it was only necessary to remove <15% of the total data collection line before the inversion process. The inverted FloaTEM data indicate a pronounced lens of freshwater that extends under the embayment toward the Sound (Fig. 7b). Along the northern end of the data collection line, fresher groundwater is indicated in the near surface sediments down to approximately 18 m depth, underlain by an apparent transition toward more saline groundwater. The profile generally becomes less resistive toward the south indicating a transition to more brackish groundwater particularly in the shallow sediments (Fig. 7b). However, the FloaTEM data show a zone of fresh waterinfluenced sediments at mid-depths that extends out toward the barrier beach and well past the tip of the eastern sandy peninsula. A direct comparison between the FloaTEM inversion and that derived from CRP data collected in April 2015 along a similar line show strong agreement in the shallow sediments (Fig. 7c), though the CRP DOI ranged from 4 to 8 m depth, including the estuary surface water column, so the vertical extent of the fresh groundwater lens was not defined.

Existing regional groundwater modeling (e.g. Walter et al., 2016, 2018) indicates that the regional freshwater/saltwater interface extends partway up the Eel River estuary from the Sound, but its position based

on these large-scale simulations is uncertain owing to a lack of field observations and calibration data. GW flowpaths that discharge in the Eel River area are subject to nutrient loading from many potential sources, including lawns and limited agriculture, golf courses, and residential septic leach fields (Howes et al., 2013; Walter et al., 2018). A recent study of groundwater-nitrate transport to the Eel River using samples collected from monitoring and pushpoint wells confirmed that fresh GW extends at least 1 km seaward from the head (northern end) of the embayment (Colman et al., 2018), though notably that study did not locate major zones of regional GW discharge. Instead they posited that submarine discharge zones of regional GW may be located farther from shore toward the center of the embayment and farther southward toward the Sound. This hypothesis is supported by the FloaTEM data that show the interpreted fresher GW lens extending to at least 2.2 km from the head of the embayment. Similar to the lowhydraulic-conductivity cap discussed in reference to the inland Rainbow Reservoir (Farmington River case study), GW/SW exchange is often inhibited in narrow nearshore areas where marine fines accumulate on the embayment bottoms, resulting in fresher GW discharge several km from shore as seen in other coastal areas (Manheim et al., 2004). FloaTEM data may provide a critical link between the point scale of direct measurements of porewater salinity in the bed sediments of embayments and the regional scale of predictions from GW flow models. The FloaTEM data could be used to guide porewater sampling with wells to focused zones of GW/SW exchange and help better characterize nutrient delivery to coastal waters.

3.6. Transferrable findings of the forward modeling and case studies

The varied field examples and forward modeling shown in this study demonstrate the utility of novel, high spatial resolution and deeply penetrating geoelectric data collected beneath larger river and estuary features that are not typically captured with conventional hydrogeological methodology. The inverted data were useful in informing a range of hydrogeologic processes, broadly binned below into three categories: (1) large-scale geology, (2) sediment-water interface sediments, and (3) fresh/saline groundwater interfaces. The utility of FloaTEM data in informing hydrogeologic investigations, along with realized challenges in data collection with the FloaTEM system, is discussed in the following.

3.6.1. Large-scale geologic structures

When FloaTEM was applied to these larger waterbody case studies, the DOI was approximately a factor of 10 greater compared to previously demonstrated towed EM and CRP systems (e.g. Briggs et al., 2019; Day-Lewis et al., 2006; Sheets and Dumouchelle, 2009) without sacrificing spatial resolution of the inverted data. This allows more holistic mapping of the aquifer system below surface water features than was previously possible, addressing a critical need of more accurate GW/SW exchange related flow and transport modeling. Our forward modeling indicated FloaTEM could readily resolve 100 Ω -m transitions in streambed resistivity at the scale of dipping geologic units (100's of m, Figs. 2 and 3) while also capturing inclusions such as clay lenses at the 50 m scale. Inversions from the Farmington River case study agree with the premise of the forward modeling, and several apparent dipping resistive bedrock layers were mapped across concurrent data collection lines at the 100's of m scale (Fig. 4). We interpret these resistive layers as sandstone interbedded in more silt-rich layers, and preliminary data indicates the sandstone may drive observed patterns in riverbank GW discharge.

The Upper Delaware River and Tallahatchie River case studies had existing geologic stratigraphy data from near-river boreholes that could be compared to the FloaTEM inversions. Along the 10.4-km Upper Delaware River reach, the 2D resistivity profile indicated several hundred-meter long zones of silt-rich substrate embedded in a coarser sand/gravel matrix overlying variable depth bedrock (Fig. 5). This

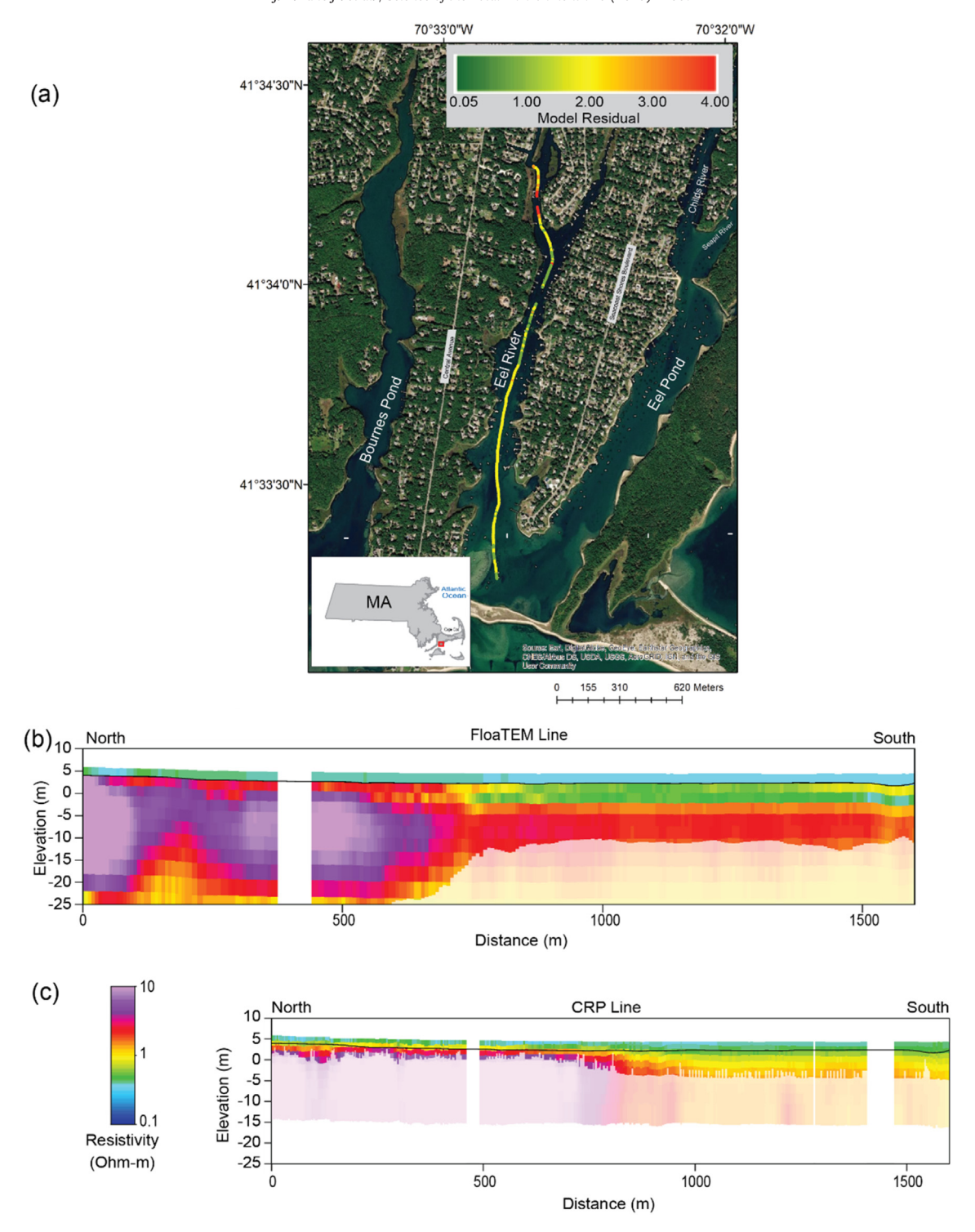


Fig. 7. The FloaTEM survey trackline plotted by inversion model data residuals is shown for the Eel River coastal estuary (a), and inverted resistivity sections from FloaTEM electromagnetic (b), and previously collected continuous resistivity profiling surveys (c).

interpretation was supported by the adjacent borehole data. Both the silt-rich and bedrock layers likely impact near surface GW connectivity and GW/SW exchange patterns by restricting flow and focusing flowpaths through the coarser bed material (Fig. 5c). Unconsolidated sediments are much thicker along the meandering Tallahatchie River study reach. There, FloaTEM data captured transitions from the higher permeability Mississippi River Valley alluvial aquifer to lower clay-rich confining units in a similar, but sharper manner to AEM data, and those sediment transitions are supported by nearby boreholes

(Fig. 6). Spatial mapping of productive aquifers vs confining units below large rivers such as this will be critical to developing more accurate predictive models of river water budgets and GW/SW exchange patterns.

3.6.2. Sediment-water interface sediments

Characterizing the distribution of coarse grained, hydraulically conductive materials versus that of fine-grained lower permeability streambed sediments is instrumental for mapping and predicting

zones of preferential GW/SW exchange. Streambed permeability is known to be a highly-sensitive model property controlling GW/SW exchange (Dai et al., 2019), and is represented by the riverbed conductance parameter in MODFLOW. Unfortunately, this parameter is typically uninformed by field data at the large reach to basin-scales in GW flow models, yielding unconstrained and uncertain model predictions. Because high electrical resistivity is indicative of sand and coarse-grained material and conductive zones are indicative of silt and clay, resistivity mapping can be used to infer sediment-water interface material types and hydraulic properties. Our forward modeling indicates that the FloaTEM system could resolve sediment-water interface sediments at the scale of several meters, but the ability to identify a fine-grained alluvial cap on more permeable bed sediments would be impacted by surface water depth and likely require a cap thickness of 2 m or more (Fig. 2). Similar thicknesses of low resistivity interface fines were mapped along the reservoir section of the Farmington River reach, a finding supported by physical observations of thick silt and organic accumulations made when the water body was partially drained in 2017 for dam maintenance (Fig. 4). Upstream, a section of resistive interface material over shallow sandstone (interpreted) bedrock coincided with a large cluster of known GW riverbank seeps.

3.6.3. Fresh/saline groundwater interfaces

The Eel River case study shown here indicates fresh submarine GW discharge, and the inverse process of saltwater intrusion, are excellent processes to target with towed TEM methods. This coastal example also suggests that the FloaTEM method would be particularly useful in mapping inland exchange zones between terrestrial rivers and natural aquifer brines, a process that can degrade surface water quality (e.g. Mast and Terry, 2019). Additionally, fresh GW discharge flowpaths embedded in brines below large rivers that are only partially captured with previous geophysical tools with limited DOI (e.g. Briggs et al., 2019) are promising targets for FloaTEM. Fresh/saline GW interfaces are often dynamic over time as their spatial distribution is driven by both paired SW/GW pressure gradients and strong subsurface density gradients. FloaTEM offers the potential for time lapse monitoring of such dynamics at single points and over repeat transects, which is not often feasible for expensive airborne AEM surveys.

3.6.4. Challenges

Typically, EM geophysical methods are considered most useful in identifying conductive targets, although examples from the Upper Delaware and Farmington Rivers indicate resistive bedrock can be successfully imaged at the formation scale. However, other types of challenges in FloaTEM data collection were identified, with coupling to infrastructure being the most serious. The effects of bridges, metallic pipelines, and overhead utilities were apparent during data collection and the proximity and extent of these features should be considered when planning a survey. Also, when towing the system, the maneuverability of the boat is impaired. Boat operators should always maintain sufficient channel width to allow turning to avoid damage to the system. However, as compared to the typical CRP system, the FloaTEM has a substantially smaller footprint, with ~10 m of equipment behind the boat as compared to 60–100 m of towed cable. Additionally, the floating frame and overhead cables of FloaTEM do not pose a propeller fouling hazard to the boat, and the system only sits <0.20 m below water surface. The complexity and volume of the data do limit the ability of the operator to perform field quality control, though preliminary inversions can be developed directly after field surveys to allow adjustment the following day. Since the field experiments were carried out in 2018, the FloaTEM system has been further developed in several ways. Firstly, the receiver coil architecture has been changed resulting in a signal to noise ratio increase of a factor of 4. This has increased the DOI to typically 100 m without sacrificing the resolution in the top 2-4 m. Secondly, the platform has been changed and it is now built of fiber frame parts that can easily be taken apart for transport. The distance between the receiver coil and the transmitter coil has been decreased by 2 m because of a new design in the transmitter minimizing some internal couplings.

4. Conclusions

As shown here with a diverse range of field case studies and forward modeling scenarios, towed time-domain EM data fill a critical need in assessing multi-scale hydrogeologic process below multi-scale waterbodies in the absence of coupling infrastructure. Specifically, the FloaTEM system was able to resolve the following two features that often impart control on spatiotemporal patterns of GW/SW exchange: 1. Bedrock layers and transitions from productive coarse grained aquifer sediments to confining units, 2. Coarse grained sediment-water interface sediments and potential paleochannels along with apparent finegrained streambed exchange- inhibiting caps. Additionally, when there is strong contrast in bed pore-water electrical conductivity such as below coastal estuaries the FloaTEM system can be used to map saltwater intrusion and discharge patterns of fresh GW. Although not tested here, it is likely the FloaTEM method will be useful in other hydrogeological settings with strong electrical contrast such as discontinuous and thawing permafrost (e.g. Walvoord and Kurylyk, 2016) where airborne methods have been deployed to good effect (Minsley et al., 2012; Rey et al., 2019). Further, as the deployment of FloaTEM is much less resource-intensive than airborne EM methods at the river reach scale (10s of km), time-lapse imaging of dynamic fresh/saline GW interface processes and storm and dam-induced riverbed exchange is feasible. Although the FloaTEM system concept is demonstrated here in several diverse case studies using Aarhus TEM technology, the basic concept is transferable to other manufacturers of similar geophysical equipment. The novel ability to map hydrologic pathways, confining units, and fresh/saline interfaces in aquatic settings where physical GW/SW exchange related methods are challenging brings needed insight into a diverse range of research- and management-related questions and will improve large-scale predictive flow modeling.

CRediT authorship contribution statement

John W. Lane: Conceptualization, Methodology, Investigation, Writing - original draft, Supervision, Funding acquisition. Martin A. Briggs: Conceptualization, Investigation, Writing - original draft, Writing - review & editing, Funding acquisition. Pradip K. Maurya: Methodology, Writing - original draft, Software. Eric A. White: Conceptualization, Methodology, Software, Writing - original draft. Jesper B. Pedersen: Methodology, Writing - original draft, Software. Esben Auken: Methodology, Writing - original draft, Software. Neil Terry: Software, Writing - original draft, Writing - review & editing. Burke Minsley: Methodology, Writing - original draft. Wade Kress: Conceptualization, Funding acquisition. Denis R. LeBlanc: Writing - original draft, Writing - review & editing. Ryan Adams: Investigation, Writing - original draft. Carole D. Johnson: Conceptualization, Methodology, Software, Writing - original draft, Writing - review & editing.

Declaration of competing interest

The authors declare that they have no known competing financial interests or personal relationships that could have appeared to influence the work reported in this paper.

Acknowledgments

This work was supported by the Innovation Fund Denmark, project rOpen (Open landscape nitrate retention mapping) and MapField (Field-scale mapping for targeted N-regulation), WATEC (Aarhus University Centre for water technology), and TOPSOIL, an Interreg project supported by the North Sea Programme of the European Regional

Development Fund of the European Union; USGS Water Availability and Use Science Program, USGS Mississippi Alluvial Plain (MAP) Project, and USGS Toxic Substances Hydrology Program.

The Farmington River data were collected for NSF grant #1824820, while the Upper Delaware River data were collected for the USGS Next Generation Water Observing Systems Program. The forward modeling and analysis were supported by DOE BER grant #DE-SC0020339. We thank Sam Banas for boat operation at the Eel River site, US National Park Service Rangers, Kevin Reish and Sean McNeil for boat support and Chris Gazoorian for logistical support at the Upper Delaware River site, Patrick McNamara for boat operation at the Farmington River site, and Shane Stocks for boat operation and photography at the Tallahatchie River site. Any use of trade, firm, or product names is for descriptive purposes only and does not imply endorsement by the U.S. Government. The various field data presented in this study are available via USGS public data release at White et al. (2020), https://doi.org/10.5066/P9E5|BAF.

References

- Auken, E., Christiansen, A.V., Westergaard, J.H., Kirkegaard, C., Foged, N., Viezzoli, A., 2009. An integrated processing scheme for high-resolution airborne electromagnetic surveys, the SkyTEM system. Explor. Geophys. 40, 184–192. https://doi.org/10.1071/FG08128
- Auken, E., Christiansen, A.V., Kirkegaard, C., Fiandaca, G., Schamper, C., Behroozmand, A.A., Binley, A., Nielsen, E., Effersø, F., Christensen, N.B., Sørensen, K., Foged, N., Vignoli, G., 2015. An overview of a highly versatile forward and stable inverse algorithm for airborne, ground-based and borehole electromagnetic and electric data. Explor. Geophys. 46, 223–235. https://doi.org/10.1071/EG13097.
- Auken, E., Foged, N., Larsen, J.J., Lassen, K.V.T., Maurya, P.K., Dath, S.M., Eiskjær, T.T., 2019. tTEM a towed transient electromagnetic system for detailed 3D imaging of the top 70 m of the subsurface. Geophysics 84, E13–E22. https://doi.org/10.1190/geo2018-0355.1.
- Bao, J., Zhou, T., Huang, M., Hou, Z., Perkins, W., Harding, S., Titzler, S., Hammond, G., Ren, H., Thorne, P., Suffield, S., Murray, C., Zachara, J., 2018. Modulating factors of hydrologic exchanges in a large-scale river reach: Insights from three-dimensional computational fluid dynamics simulations. Hydrol. Process. 32, 3446–3463. https://doi.org/10.1002/hyp.13266.
- Barclay, J.R., 2019. Imprints of the Land: Spatial and Temporal Connections Between Land Use and Water Quality. Doctoral Thesis. University of Connecticut.
- Bianchin, M.S., Smith, L., Beckie, R.D., 2011. Defining the hyporheic zone in a large tidally influenced river. J. Hydrol. 406, 16–29. https://doi.org/10.1016/j.jhydrol.2011.05.056.
- Boano, F., Harvey, J.W., Marion, A., Packman, A.I., Revelli, R., Ridolfi, L., Worman, A., 2014. Hyporheic flow and transport processes: mechanisms, models, and biogeochemical implications. Rev. Geophys., 1–77 https://doi.org/10.1002/2012RG000417.
- Briggs, M.A., Voytek, E.B., Day-Lewis, F.D., Rosenberry, D.O., Lane, J.W., 2013. Understanding water column and streambed thermal refugia for endangered mussels in the delaware river. Environ. Sci. Technol. 47, 11423–11431. https://doi.org/10.1021/es4018893.
- Briggs, M.A., Nelson, N., Gardner, P., Solomon, D.K., Terry, N., Lane, J.W., 2019. Wetland-scale mapping of preferential fresh groundwater discharge to the Colorado River. Groundwater https://doi.org/10.1111/gwat.12866.
- Briggs, M.A., Tokranov, A.K., Hull, R.B., LeBlanc, D.R., Haynes, A.B., Lane, J.W., 2020. Hill-slope groundwater discharges provide localized stream ecosystem buffers from regional per- and polyfluoroalkyl substances (PFAS) contamination. Hydrol. Process. https://doi.org/10.1002/hyp.13752.
- Burton, B.L., Minsley, B.J., Bloss, B.R., Kress, W.H., Rigby, J.R., Smith, B.D., 2020. High-resolution airborne geophysical survey of the Shellmound, Mississippi area. U.S. Geol. Surv. Sci. Investig. Map 3449 2 sheets. https://doi.org/10.3133/sim3449.
- Christiansen, A.V., Auken, E., 2012. A global measure for depth of investigation. Geophysics 77, WB171–WB177.
- Colman, J.A., LeBlanc, D.R., Böhlke, J.K., McCobb, T.D., Kroeger, K.D., Belaval, M., Cambareri, T.C., Pirolli, G.F., Brooks, T.W., Garren, M.E., Stover, T.B., Keeley, A., 2018. Geochemical conditions and nitrogen transport in nearshore groundwater and the subterranean estuary at a Cape Cod embayment, East Falmouth, Massachusetts, 2013–14. US Geol. Surv. Sci. Investig. Rep. 2018–5095, 69. https://doi.org/10.3133/sir20185095.
- Dai, H., Chen, X., Ye, M., Song, X., Hammond, G., Hu, B., Zachara, J.M., 2019. Using Bayesian networks for sensitivity analysis of complex biogeochemical models. Water Resour. Res. 55, 3541–3555. https://doi.org/10.1029/2018WR023589.
- Day-Lewis, F.D., White, E.A., Johnson, C.D., Lane, J.W., Belaval, M., 2006. Continuous resistivity profiling to delineate submarine groundwater discharge examples and limitations. Lead. Edge (Tulsa, OK) 25, 724–728. https://doi.org/10.1190/1.2210056.
- Harbaugh, A.W., Banta, E.R., Hill, M.C., McDonald, M.G., 2000. MODFLOW-2000, the U.S. Geological Survey modular ground-water models; user guide to modularization concepts and the ground-water flow process. U.S. Geol. Surv. Open File Rep. 121.
- Hare, D.K., Briggs, M.A., Rosenberry, D.O., Boutt, D.F., Lane, J.W., 2015. A comparison of thermal infrared to fiber-optic distributed temperature sensing for evaluation of groundwater discharge to surface water. J. Hydrol. 530, 153–166. https://doi.org/ 10.1016/j.jhydrol.2015.09.059.

- Harvey, J.W., Gooseff, M.N., 2015. River corridor science: hydrologic exchange and ecological consequences from bedforms to basins. Water Resour. Res. 51, 1–30. https://doi.org/10.1002/2015WR017617.
- Harvey, M., Briggs, M.A., Dawson, C.B., White, E.A., Fosberg, D., Haynes, A., Moore, E., 2019. Thermal Infrared and Photogrammetric Data Collected by Small Unoccupied Aircraft System for the Evaluation of Wetland Restoration Design at Tidmarsh Wildlife Sanctuary, Plymouth, Massachusetts. USA. U.S. Geol. Surv. public data release https://doi. org/10.5066/P9X8PBWN.
- Hatch, M., Munday, T., Heinson, G., 2010. A comparative study of in-river geophysical techniques to define variations in riverbed salt load and aid managing river salinization. Geophysics 75. https://doi.org/10.1190/1.3475706.
- Hester, E.T., Gooseff, M.N., 2010. Moving beyond the banks: hyporheic restoration is fundamental to restoring ecological services and functions of streams. Environ. Sci. Technol. 44, 1521–1525. https://doi.org/10.1021/es902988n.
- Hoffmann, J.P., 2017. Thickness of the Mississippi River Valley alluvium and its relationship to the underlying Tertiary formations of northwestern Mississippi. Mississippi Department of Environmental Quality Office of Geology Open-file Report. 291.
- Howes, B., Samimy, R., Schlezinger, D., Eichner, E., Kelley, S., Ramsey, J., Detjens, P., 2013. Linked Watershed-embayment Approach to Determine Critical Nitrogen Loading Thresholds for the Waquoit Bay and Eel Pond Embayment Systems, Towns of Falmouth and Mashpee, Massachusetts. Massachusetts Estuaries Proj. Final Rep (205 p.).
- Hull, R.B., Johnson, C.D., Stone, B.D., LeBlanc, D.R., McCobb, T.D., Phillips, S.N., Pappas, K.L., Lane, J.W., 2019. Lithostratigraphic, geophysical, and hydrogeologic observations from a boring drilled to bedrock in glacial sediments near Nantucket sound in East Falmouth, Massachusetts. U.S. Geol. Surv. Sci. Investig. Rep. vols. 2019–5042. https://doi.org/10.3133/sir20195042 27 p.
- Kalbus, E., Reinstorf, F., Schirmer, M., 2006. Measuring methods for groundwater, surface water and their interactions: a review. Hydrol. Earth Syst. Sci. Discuss. 3, 1809–1850. https://doi.org/10.5194/hessd-3-1809-2006.
- Kalisperi, D., Kouli, M., Vallianatos, F., Soupios, P., Kershaw, S., Lydakis-Simantiris, N., 2018. A transient electromagnetic (TEM) method survey in north-central coast of crete, Greece: evidence of seawater intrusion. Geosci 8. https://doi.org/10.3390/geosciences8040107.
- Kress, W.H., Clark, B., Barlow, J., 2018. Coupling modeling with mapping to assess water availability in the Mississippi Alluvial Plain. In Proceedings SAGEEP. Nashville,
- Kwon, H.-S., Kim, J.-H., Ahn, H.-Y., Yoon, J.-S., Kim, K.-S., Jung, C.-K., Lee, S.-B., Uchida, T., 2005. Delineation of a fault zone bedeath a riverbed by an electrical resistivity survey using a floating streamer cable. Explor. Geophys. 36, 50–58.
- Madsen, L.M., Lassen, K.V., Auken, E., Christiansen, A.V., 2017. Comparison of near-surface sensitivity functions of airborne and ground-based EM systems. Second European Airborne Electromagnetics Conference. European Association of Geoscientists & Engineers, pp. 1–5. https://doi.org/10.3997/2214-4609.201702150.
- Manheim, F.T., Krantz, D.E., Bratton, J.F., 2004. Studying ground water under delmarva coastal bays using electrical resistivity. Ground Water 42, 1052–1068. https://doi.org/10.1111/j.1745-6584.2004.tb02643.x.
- Marazuela, M.A., Vázquez-Suñé, E., Custodio, E., Palma, T., García-Gil, A., Ayora, C., 2018. 3D mapping, hydrodynamics and modelling of the freshwater-brine mixing zone in salt flats similar to the Salar de Atacama (Chile). J. Hydrol. 561, 223–235. https://doi.org/10.1016/j.jhydrol.2018.04.010.
- Marazuela, M.A., Vázquez-Suñé, E., Ayora, C., García-Gil, A., Palma, T., 2019. The effect of brine pumping on the natural hydrodynamics of the Salar de Atacama: the damping capacity of salt flats. Sci. Total Environ. 654, 1118–1131. https://doi.org/10.1016/j.scitotenv.2018.11.196.
- Mast, A., Terry, N., 2019. Controls on spatial and temporal variations of brine discharge to the Dolores River in the Paradox Valley, Colorado, 2016–18. US Geol. Surv. Sci. Investig. Rep., 2019–5058 https://doi.org/10.3133/sir20195058.
- McLachlan, P.J., Chambers, J.E., Uhlemann, S.S., Binley, A., 2017. Geophysical characterisation of the groundwater–surface water interface. Adv. Water Resour. 109, 302–319. https://doi.org/10.1016/j.advwatres.2017.09.016.
- Minsley, B.J., Abraham, J.D., Smith, B.D., Cannia, J.C., Voss, C.I., Jorgenson, M.T., Walvoord, M.a., Wylie, B.K., Anderson, L., Ball, L.B., Deszcz-Pan, M., Wellman, T.P., Ager, T.a., 2012. Airborne electromagnetic imaging of discontinuous permafrost. Geophys. Res. Lett. 39, 1–8. https://doi.org/10.1029/2011GL050079.
- Mollidor, L., Tezkan, B., Bergers, R., Löhken, J., 2013. Float-transient electromagnetic method: in-loop transient electromagnetic measurements on Lake Holzmaar, Germany. Geophys. Prospect. 61, 1056–1064. https://doi.org/10.1111/1365-2478.12025.
- Munk, L., Hynek, S., Bradley, D., Boutt, D., Labay, K., Jochens, H., 2016. Lithium brines: a global perspective. Rev. Econ. Geol. 18, 339–365.
- Nyquist, J.E., Freyer, P.A., Toran, L., 2008. Stream bottom resistivity tomography to map ground water discharge. Ground Water 46, 561–569. https://doi.org/10.1111/j.1745-6584.2008.00432.x.
- Olcott, P.G., 1995. Connecticut, Maine, Massachusetts, New Hampshire, New York, Rhode Island, Vermont, HA 730-M. Groundwater Atlas of the US. United States Geological Survey.
- Ong, J.B., Lane, J.W., Zlotnik, V.a., Halihan, T., White, E.a., 2010. Combined use of frequency-domain electromagnetic and electrical resistivity surveys to delineate near-lake groundwater flow in the semi-arid Nebraska Sand Hills, USA. Hydrogeol. J. 18, 1539–1545. https://doi.org/10.1007/s10040-010-0617-x.
- Palacky, G.J., 1988. Resistivity characteristics of geologic targets. In: Nabighian, M.N. (Ed.), Investigations in Geophysics Vol. 3: Electromagnetic Methods in Applied Geophysics-Theory. 1. Soc. Expl. Geophys, pp. 53–129.
- Parsekian, A.D., Singha, K., Minsley, B.J., Holbrook, W.S., Slater, L., 2014. Multiscale geophysical imaging of the critical zone. Rev. Geophys. 53, 1–26. https://doi.org/10.1002/2014RG000465.

- Poole, G.C., 2010. Stream hydrogeomorphology as a physical science basis for advances in stream ecology. J. N. Am. Benthol. Soc. 29, 12–25. https://doi.org/10.1899/08-070.1.
- Rey, D.M., Walvoord, M., Minsley, B., Rover, J., Singha, K., 2019. Investigating lake-area dynamics across a permafrost-thaw spectrum using airborne electromagnetic surveys and remote sensing time-series data in Yukon Flats, Alaska. Environ. Res. Lett. 14. https://doi.org/10.1088/1748-9326/aaf06f.
- Rosenberry, D.O., Briggs, M.A., Voytek, E.B., Lane, J.W., 2016. Influence of groundwater on distribution of dwarf wedgemussels (Alasmidonta heterodon) in the upper reaches of the Delaware River, northeastern USA. Hydrol. Earth Syst. Sci. 20, 1–17. https:// doi.org/10.5194/hess-20-1-2016.
- Sanford, W.E., Pope, J.P., 2013. Quantifying groundwater's role in delaying improvements to Chesapeake Bay water quality. Environ. Sci. Technol. 47, 13330–13338. https://doi. org/10.1021/es401334k.
- Sheets, R.A., Dumouchelle, D.H., 2009. Geophysical Investigation Along the Great Miami River From New Miami to Charles M. Bolton Well Field. Ohio. U.S. Geol. Surv. Open File Rep. 2009–1025. Circinnati
- Slater, L.D., Ntarlagiannis, D., Day-Lewis, F.D., Mwakanyamale, K., Versteeg, R.J., Ward, A., Strickland, C., Johnson, C.D., Lane, J.W., 2010. Use of electrical imaging and distributed temperature sensing methods to characterize surface water-groundwater exchange regulating uranium transport at the Hanford 300 Area, Washington. Water Resour. Res. 46, 1–13. https://doi.org/10.1029/2010WR009110.
- Soller, D., Packard, P.H., Garrity, C.P., 2012. Database for USGS Map I-1970- map showing the thickness and character of Quaternary sediments in the glaciated United States east of the Rocky Mountains (Report No. 656). U.S. Geol. Surv. Data Serries. https:// pubs.usgs.gov/ds/656/
- Tesoriero, A.J., Saad, D. a, Burow, K.R., Frick, E. a, Puckett, L.J., Barbash, J.E., 2007. Linking ground-water age and chemistry data along flow paths: implications for trends and transformations of nitrate and pesticides. J. Contam. Hydrol. 94, 139–155. https://doi.org/10.1016/j.jconhyd.2007.05.007.

- Thompson Jobe, J.A., Gold, R.D., Briggs, R.W., Williams, R.A., Stephenson, W.J., Delano, J.E., Shah, A., Minsley, B., 2020. Evidence for late Quaternary deformation along Crowleys Ridge, New Madrid seismic zone. Tectonics 39. https://doi.org/10.1029/2019TC005746.
- Toran, L., Johnson, M., Nyquist, J., Rosenberry, D., 2010. Delineating a road-salt plume in lakebed sediments using electrical resistivity, piezometers, and seepage meters at Mirror Lake, New Hampshire, U.S.A. Geophysics 75. https://doi.org/10.1190/
- Uchupi, E., Oldale, R.N., 1994. Spring sapping origin of the enigmatic relict valleys of Cape Cod and Martha's Vineyard and Nantucket Islands, Massachusetts. Geomorphology 9. https://doi.org/10.1016/0169-555X(94)90068-X.
- Walter, D.A., Mccobb, T.D., Masterson, J.P., Fienen, M.J., 2016. Potential effects of sea-level rise on the depth to saturated sediments of the Sagamore and Monomoy flow lenses on Cape Cod, Massachusetts. US Geol. Surv. Sci. Investig. Rep. 55, 2016–5058. https://doi.org/10.3133/sir20165058.
- Walter, D.A., McCobb, T.D., Fienen, M.N., 2018. Use of a numerical model to simulate the hydrologic system and transport of contaminants near joint base Cape Cod, Western Cape Cod, Massachusetts. Sci. Investig. Rep. 2018–5139.
- Walvoord, M.A., Kurylyk, B.L., 2016. Hydrologic impacts of thawing permafrost a review. Vadose Zo. J., 156 https://doi.org/10.2136/vzj2016.01.0010.
 White, E.A., Johnson, C.D., Briggs, M.A., Adams, R.F., Stocks, S.J., Minsley, B.J., Kress, W.H.,
- White, E.A., Johnson, C.D., Briggs, M.A., Adams, R.F., Stocks, S.J., Minsley, B.J., Kress, W.H., Rigby, J.R., Lane Jr., J.W., 2020. Floating and Towed Transient Electromagnetic Surveys used to Characterize Hydrogeology underlying Rivers and Estuaries: March – December 2018: U.S. Geological Survey data release. https://doi.org/10.5066/P9E5JBAF.
- ber 2018: U.S. Geological Survey data release. https://doi.org/10.5066/P9E5JBAF. Winter, T.C., Harvey, J.W., Franke, O.L., Alley, W.M., 1998. Ground water and surface water: a single resource. U. S. Geol. Surv. Circ. 1139, 79.
- Wolock, D.M., 2003. Flow characteristics at U.S. Geological Survey stream gages in the conterminous United States, U.S. Geol. Surv. Open-File Rep. 03–146 (Digit. data set).